Turbulence Measurements in an Ejector Wing Flow Field

by

G. D. Catalano
Louisiana State University
Baton Rouge, Louisiana

H. E. Wright and D. Stevens
Air Force Institute of Technology
Wright Patterson AFB, Ohio

K. S. Nagaraja
AF Wright Aeronautical Labs
Wright Patterson AFB, Ohio

For presentation at the Ejector Workshop for Aerospace Applications, August 3-5, 1981, Dayton, Ohio

DISCLAIMER NOTICE

THIS DOCUMENT IS BEST QUALITY PRACTICABLE. THE COPY FURNISHED TO DTIC CONTAINED A SIGNIFICANT NUMBER OF PAGES WHICH DO NOT REPRODUCE LEGIBLY.

I. Introduction

Consider the principle of an ejector[1]. In the simplest cast, coaxial jets are confined to a duct rather than a constant pressure atmosphere. For this flow field, the mass flow rate averaged mean axial momentum is not conserved and the static pressure may vary with downstream location. There will be an increase of pressure with increasing downstream position as the jet cores are being consumed by rapid shear layer mixing. In fact, the pressure may also continue to rise in the developing flow zone downstream of the disappearance of the cores. This pressure rise can be considered the source of the pumping effect of the ejector.

Significant and fundamental developments in thrust augmenting ejectors have been accomplished in the last several years. Hypermixing nozzles have been developed with a resultant increase in ejector compactness realized[2]. Mixing and diffusion of flows have been achieved simultaneously with performance advantage. Thrust augmentation ratios on the order of two in an ejector of inlet area ratio 23 have been achieved experimentally[3]. A theoretical methodology which can evaluate the performance of the ejectors subject to a wide range of variation in the thermodynamic parameters of the injected and the entrained fluids has been developed for incompressible and compressible flows for a constant area duct[4]. High lift characteristics of an ejector-flapped wing have been evaluated[5]. A numerical prediction of three dimensional ejector flows has been proposed[6].

Although the literature on ejectors in general and, particularly, thrust augmenting ejectors, is quite extensive, the turbulence field has been essentially ignored. The information that is available is predominantly concerned with flows in constant area pipes with Razinley and

Brighton[7] presenting an extensive set of one point statistical measurements for varying mean velocity ratios and jet/pipe diameter ratios.

The purpose of this investigation is to conduct an extensive survey of the resultant velocity flow field of a given ejector wing design. The effectiveness of the ejector will be assessed by comparing the flow field with the ejector powered and with the ejector unpowered. The data in this experiment is obtained by use of a laser velocimeter in conjunction with a photon correlation processing technique. Photon counting offers improved system sensitivity by permitting velocity measurements to be made even when insufficient signal photons are available to define a classical scattering signal. When required for an improved signal to noise ratio, the naturally occuring contaminant particles are augmented by kerosene vapor. The use of the kerosene vapor allows a flow visualization technique to be employed as well.

The relevance of this investigation is reinforced by one of the major conclusions of the Workshop in 1979 which is that a significant amount of basic research using smaller models (cold or hot air supply) and analytical development should be continued vigorously for both static and at airpeed conditions[8].

II. Experimental Equipment and Technique

The facility used for this investigation is a two dimensional smoke tunnel. This facility employs an open return system of flow, capable of subsonic incompressible velocities up to 23 meters/second, using two diffuser isolated 1.5 horsepower motor driven fans. All measurements are taken at a nominal freestream velocity of 8 m/sec. The velocity was monitored at first by a Prandtl type pitot probe and a microamanometer.

These were later discarded in favor of the laser velocimeter as a means of setting and checking the freestream velocity.

The removable front test section measures 1.5 m in length, 1.0 m in height and 0.07 m in width. The back wall of the test section is of laminated plate glass, whereas the front wall is of 0.0097 m thick plexiglass. This window arrangement is acceptable in light of the fact that the laser velocimeter is operated in the backscatter mode. The test section is noted as having a downhill gradient of 0.05 m in 1.5 m.

The flow marker particles are introduced into the flow system in thin streamtubes by a stack and injector apparatus, positioned in the tunnel contraction region. The stack is of airfoil shape with sixty five 0.60 cm inside diameter injector tubes issuing from it. The marker particles are generated in a process where, two 900 watt inconel heaters boil kerosene fuel at 605 degrees Kelvin, creating vapor particles that are then mixed under turbulent conditions with cool air to produce a dense white nontoxic and noncorrosive smoke. Water vapor is condensed out of the smoke in a condensing chamber prior to entrance into the stack/injector apparatus, thereby eliminating water condensation in the injector tubes and the test section.

A great deal of effort was spent in reducing turbulence levels in this flow system. These efforts included installatior of a 0.2 m radius bell mouth to the tunnel inlet, in an attempt to correct for a low concentration ratio of 11.5 to 1.0. Immediately downstream of this location a 0.076 m thick section of honeycomb, with a cell length to diameter ratio of 8.0, was installed to reduce large scale turbulent structures. In addition a series of screens (progressively finer downstream) were mounted prior to the stack/injector location. From measurements taken in the freestream, it would appear that turbulent intensities approach a value

of 0.01 in the smoke streamtubes. These values must be attributed to the shape of the stack/injector system, its location and the process of issuing a secondary flow into the mainstream through the injectors.

The specific flow field investigated is an ejector wing design conceived by Vought under contract with the Flight Dynamics Laboratory at Wright Patterson AFB (Figure 1)[9]. A two dimensional model is constructed and placed in the test section of the wind tunnel. The ejector plenum is supplied from the laboratory compressed air reservoir. The design of the ejector is presented in Figure 2. Considerable effort was expended in attempting to achieve a uniform exit velocity profile with relatively low values of the turbulent intensities. The aspect ratio of the rectangular nozzle is 4.1:1 and the solidity ratio is 0.327:1. The mean velocity at the nozzle exit plane, U_2, is kept at a constant 16 m/sec.

The laser used for all measurements is a Helium-Neon Laser of 15 milliwatts intensity at 6328.0×10^{-10} m, plus associated power unit. The laser beam diameter is 1.1 m at the $1/e^2$ points. The transmitting optics consisted of a transmitter beamsplitter and polarization unit mounted to the laser head, a frequency shifting electro-optic phase modulating crystal, two front surface silvered plane mirrors mounted at 45 degrees to the horizontal and a convex focussing lens of 100 cm focal length. The beamsplitter takes the incident beam from the laser and divides it into two equal intensity, 1.1 mm diameter beams.

The frequency shifting phase modulator is required in the optical train to eliminate any flow direction sense ambiguities and provide measurements in regions of high turbulent intensity. In principle a uniform shifting of the fringes in the control volume (point of laser beam intersection) is possible with an application of a sawtooth voltage to

the phase modulator's two electro-optical crystals. A resulting increase or decrease in the doppler frequency of the flow enables the flow direction to be determined. A drive unit is required for the phase modulator unit as well as a frequency counter for accurate determination of the doppler frequency shift applied.

The electronic processing scheme is composed of a digital photon correlator and data storage unit, associated power supply and oscilliscope for visual observation of the autocorrelation function growth with time. The correlator possesses a resolution time of from 50 nanoseconds to 1 second. Measurements were taken in the single clipped autocorrelation mode and at an infinite sample rate.

Special note should be made of the turbulent intensities measurement technique. Care is taken in order to minimize the problems of background flare light and photon pileup. The effects of these two phenomena can result in a skewness or a distortion of the photon correlation function from which the mean velocity and local turbulent intensity are calculated. Therefore a numerical technique[10] is employed which results in the alleviation of the skewness problem.

III. Experimental Results and Discussion

A. Flow Visualization

A series of photographs depicting qualitatively the resultant flow field about the ejector wing model as shown in Figure 3 through 9. For all photographs the ratio between the ejector exit plane mean velocity, U_2, and the tunnel speed, V, is equal to 2:1. The angle of attack, α, between the wing model chord line and the incoming tunnel flow is varied from -5° to $+25^{\circ}$. For each value of α, the case with the ejector powered

and the unpowered case are examined.

By examining each set of figures, three general observations are made concerning the effects of the ejector. First, significantly more smoke (hence, tunnel airflow) is entrained into the constant area duct between the lower and upper airfoils in the powered case. In fact, it appears that near stagnation conditions are reached downstream of the nozzle with jet flow off. Secondly, with the ejector powered, there is an increase in curvature of the streamlines in the vicinity of the leading edge stagnation point. As will be discussed later in this report, this is evidence of the shift of the wing model's stagnation point further downstream on the lower surface of the front airfoil. Thirdly, the smoke streamlines above the wing are shifted downward towards the airfoil surface in the powered case. Thus, qualitative evidence exists that one of the effects of the ejector is to decrease the resultant wake flow behind the wings.

B. Mean Velocities and Turbulent Intensities

In Figure 10, the location of the mean velocity and turbulent intensity data obtained are shown. Note that in all cases, x is measured, longitudinally, from the leading edge and z is measured vertically from the airfoil surfaces.

Turbulent intensity is defined here as the ratio between the root mean square of the velocity fluctuations, u_{rms}, non-dimensionalized by the local mean velocity, U.

Figure 11 shows mean velocity profiles upstream of the ejector wing while the turbulent intensity profiles are presented in Figure 12. The effect of the ejector shown in the mean velocity profiles is to accelerate the mean flow above the upper surface and to decelerate the mean flow beneath the ejector wing. This effect is quite pronounced immediately

upstream of the leading edge. The turbulent intensities are not as well behaved but the value of u_{rms}/U does seem to increase above the upper surface with the ejector powered.

Mean velocity and turbulent intensity profiles are shown for the downstream locations x/c = 0.2, (F), and x/c = 0.5, (I), in Figures 13 and 14. Both these locations are above the upper surface and the mean flow is consistently faster in the ejector powered case. The turbulent intensity data reinforces an observation made with reference to flow visualization evidence. The value of the turbulent intensities reduce to the free stream value closer to the wing surface with the ejector working. This would again indicate a shift of the potential flow down toward the upper surface.

Consider the data presented for the lower surface locations for x/c = .02, x/c = .04, and x/c = 0.2. In figures 15 through 17, at each flow location, the mean longitudinal velocity, U, is less in the powered case. This suggests the movement of the stagnation further along the lower surface as can be argued from Figure 18. As the stagnation point moves downstream, the apparent angle of attack of the airfoil will increase. With the increase of α, the mean velocity measured in the longitudinal direction will necessarily decrease close to the stagnation point.

The mean and turbulent velocity field downstream of the ejector nozzle is examined in Figures 19 through 21 for x/c = 0.44, 0.58, and 0.72. Note that the flow for both cases actually accelerates after it enters the constant area mixing duct. Also consider the relatively high turbulent intensities in the confining duct for the ejector powered case. Values of u_{rms}/U equal to 0.25 are measured which is indicative of jet mixing rather than characteristic of duct type flow. Once again for the field above the wing, the velocity returns to the free stream turbulence

condition faster with the jet working. For example, for z = 10 cm in Figure 21, u_{rms}/U is equal to .05 for the nonpowered case but possesses a value of .01 for the ejector working case.

IV. Summary

An experimental investigation of the resultant turbulent flow field about an ejector wing design incorporating a constant area mixing duct is made. Mean velocities and turbulent intensities are calculated from the photon correlation functions. Comparison between the ejector powered and non-powered cases are made. Qualitative information as well is obtained from a flow visualization technique. The following results are obtained.

1) The ejector consistently accelerated the flow field above the wings' upper surface. The influence is felt upstream of the model's leading edge.

2) The stagnation point moved further downstream along the lower surface for the ejector powered case, indicating an apparent increase in the effective angle of attack.

3) The turbulent intensities in the confining duct are more indicative of free or coaxial jet turbulence levels.

4) The streamlines above the wing's upper surface are compressed downwards toward the airfoil indicating a reduction in the turbulence and, hence, the wake region.

References

1. Johnston, J. P., "Internal Flows", Turbulence ed. P. Bradshaw, Topics in Applied Physics, Vol. 12, Springer-Verlag, New York, 1978, pp. 154-157.

2. Quinn, B., "Compact Ejector Thrust Augmentation", J. Aircraft, Vol. 10, No. 8, August 1973.

3. Quinn, B., "Experiments with Hypermixing Nozzles in an Area Ratio 23 Ejector, ARL 72-0084, June 1972.

4. Nagaraja, K. S., Hammond, D. L., and Graetch, J. E., "One Dimensional Compressible Ejector Flows", AIAA Paper 73-1184, Nov. 1973.

5. Woolard, H. W., "Thin Airfoil Theory of an Ejector-Flapped Wing Section", J. Aircraft, Vol. 12, Jan. 1975.

6. Roberts, D. W. and Paynter, G. C., "Numerical Prediction of 3-D Ejector Flows", Workshop on Thrust Augmenting Ejectors, Ames Research Center, Moffett Field, California, June 28-29, 1978, pp. 55-70.

7. Razinsky, E., and Brighton, J. A., "Confined Jet Mixing for Nonseparating Conditions", Trans ASME, D, Vol. 93, September, 1971, pp. 333-349.

8. Koenig, D. G., "NASA Overview", Workshop on Thrust Augmenting Ejectors, Ames Research Center, Moffett Field, California, June 28-29, 1978, pp. 23-40.

9. Ejector Wing Design, Vought Corporation Advanced Technology Center, ATC Report No. R-91100/9CR-44, September 1979.

10. Catalano, G. D., Walterick, R. E., and Wright, H. E., "Improved Measurement of Turbulent Intensities by Use of Photon Correlation", AIAA Journal.

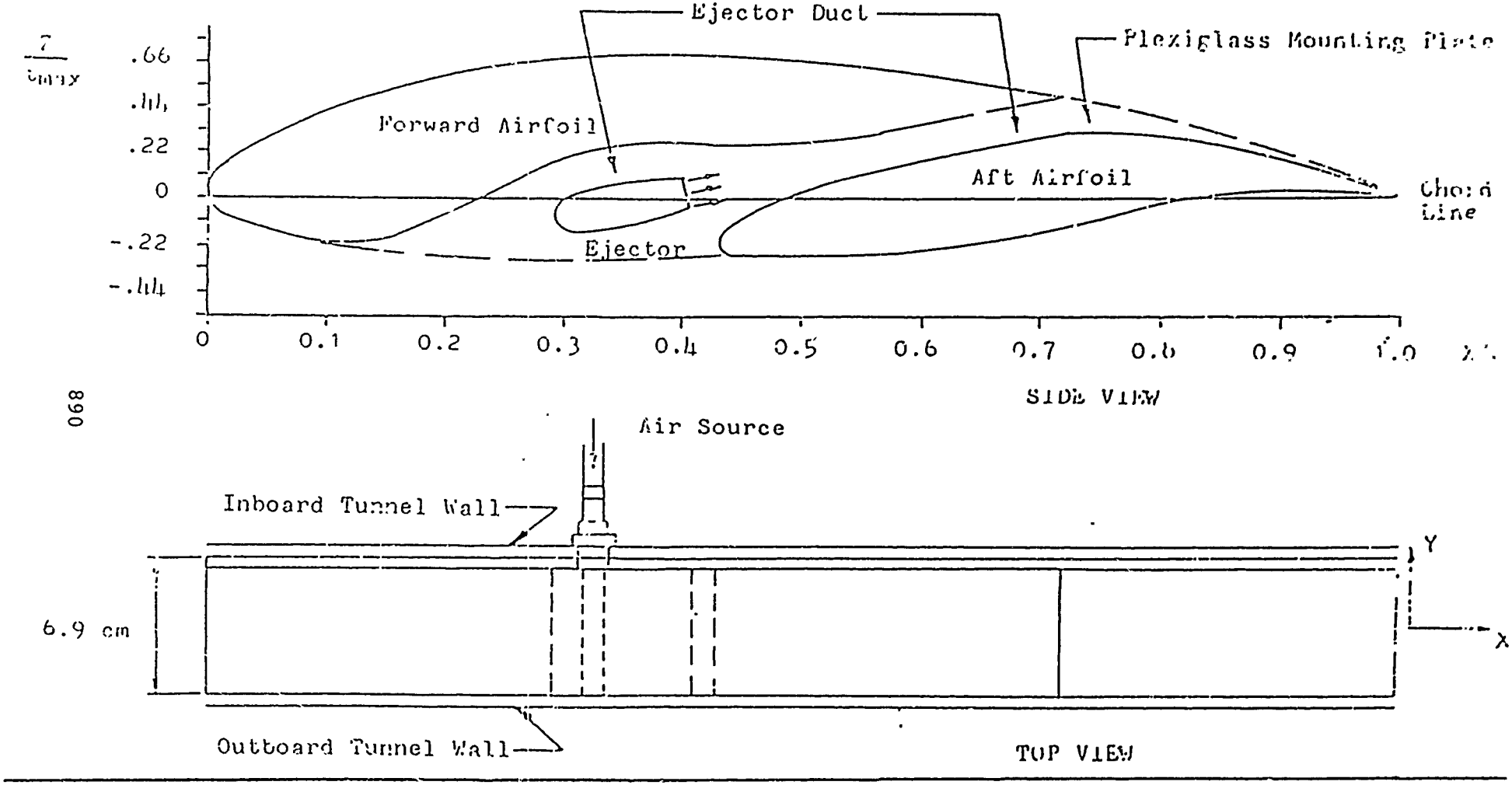

890

Figure 1. Ejector Wing Design
Chord Length, C, = 58.1 cm
Maximum thickness, t_m, = 11.1 cm

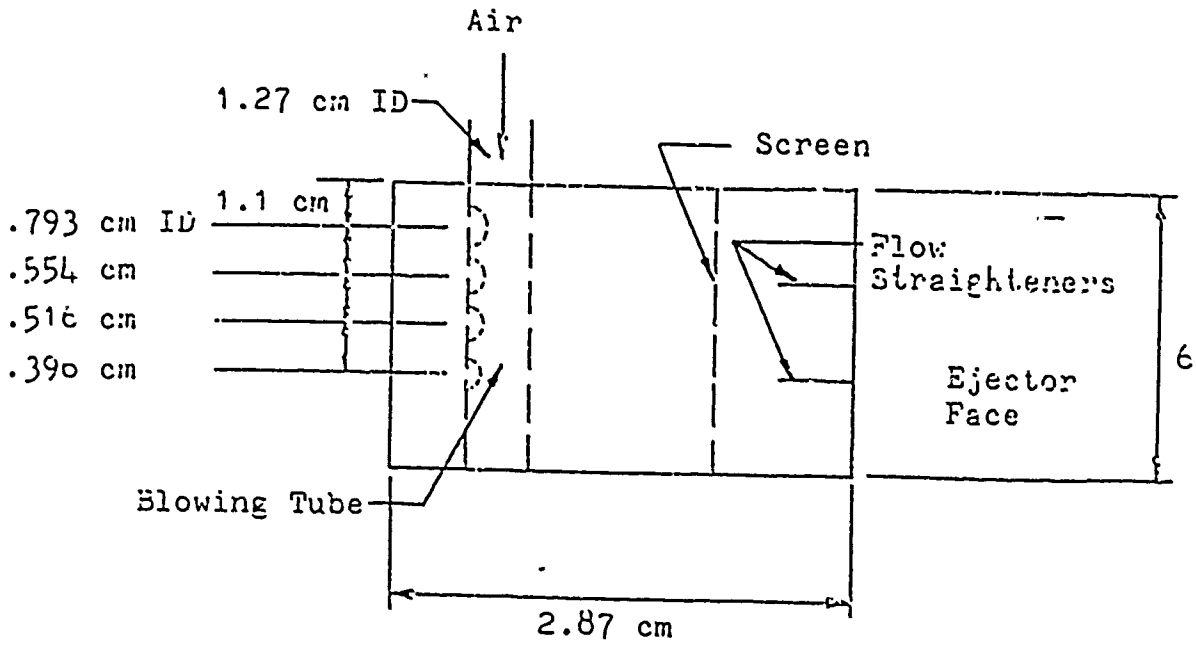

TOP VIEW

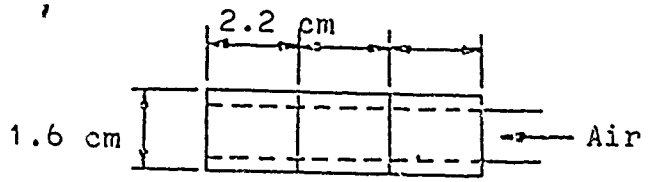

Ejector Face Area = 10.66 cm^2

FRONT VIEW

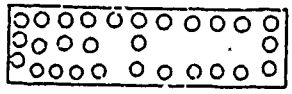

225 holes

.132 cm ID each

Screen Hole Area = 3.49 cm^2

SCREEN

Figure 2. EJECTOR 891

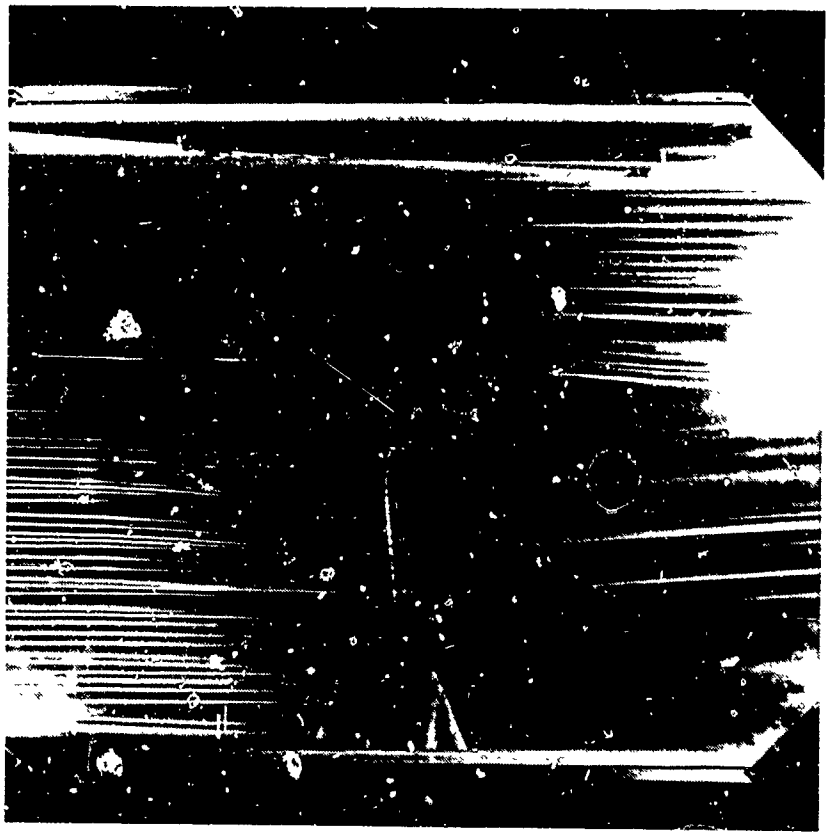

Unpowered

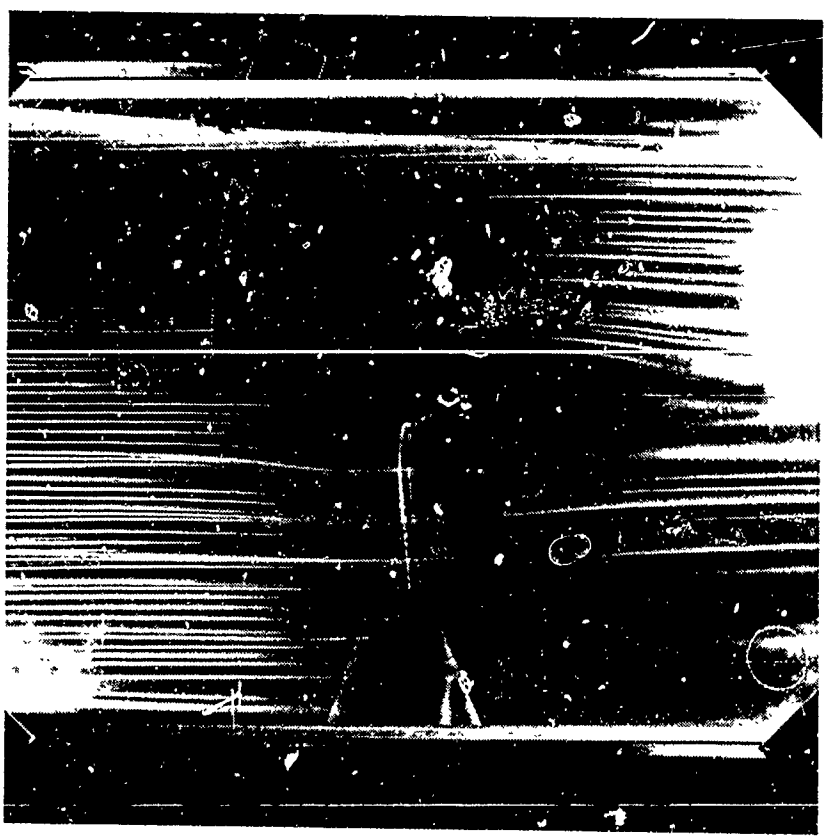

Powered

Figure 3. Flow Visualization for $\alpha = -5^{o}$.

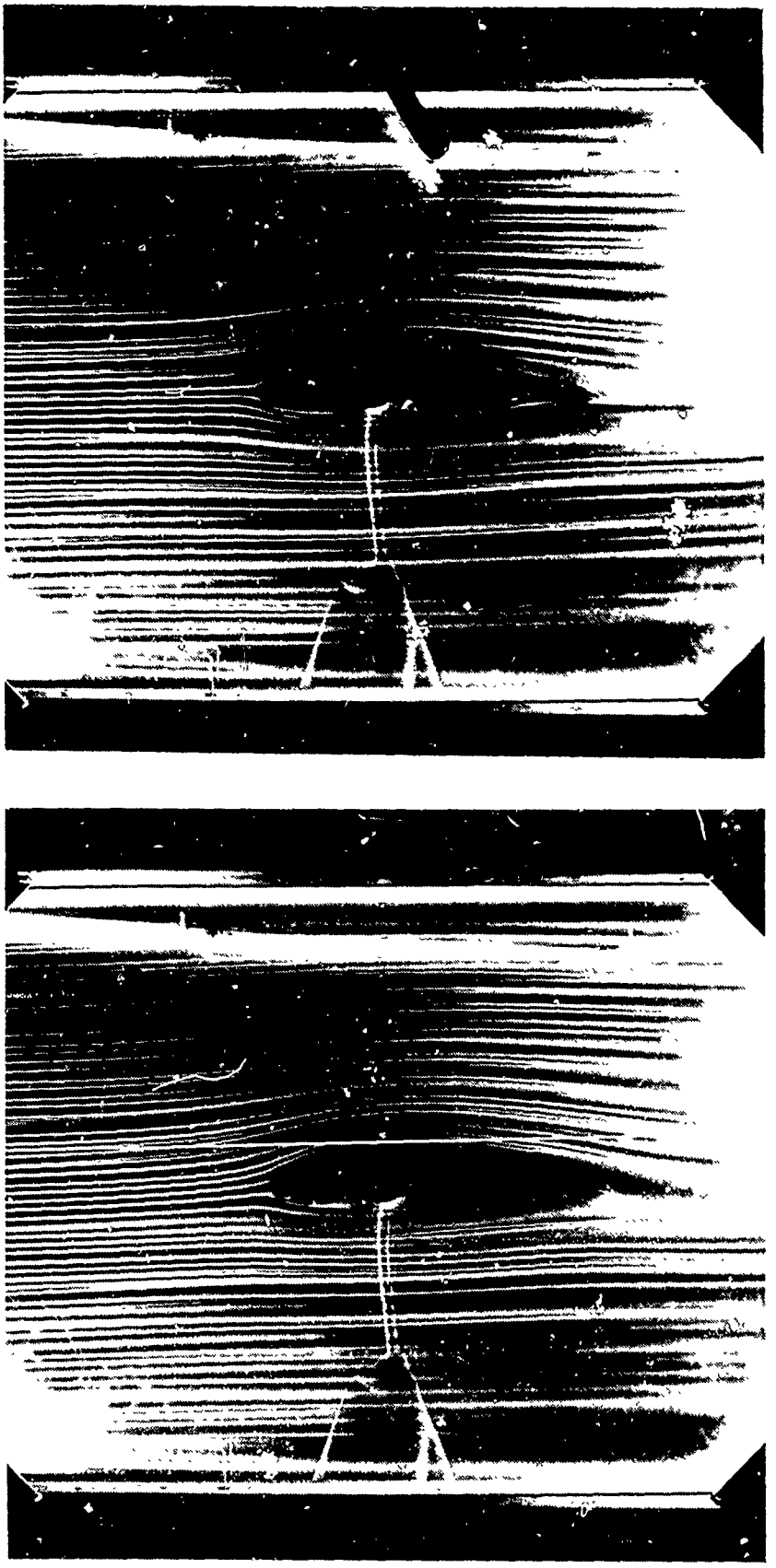

Unpowered

Powered

Figure 4. Flow Visualization for $\alpha = 0^{\circ}$.

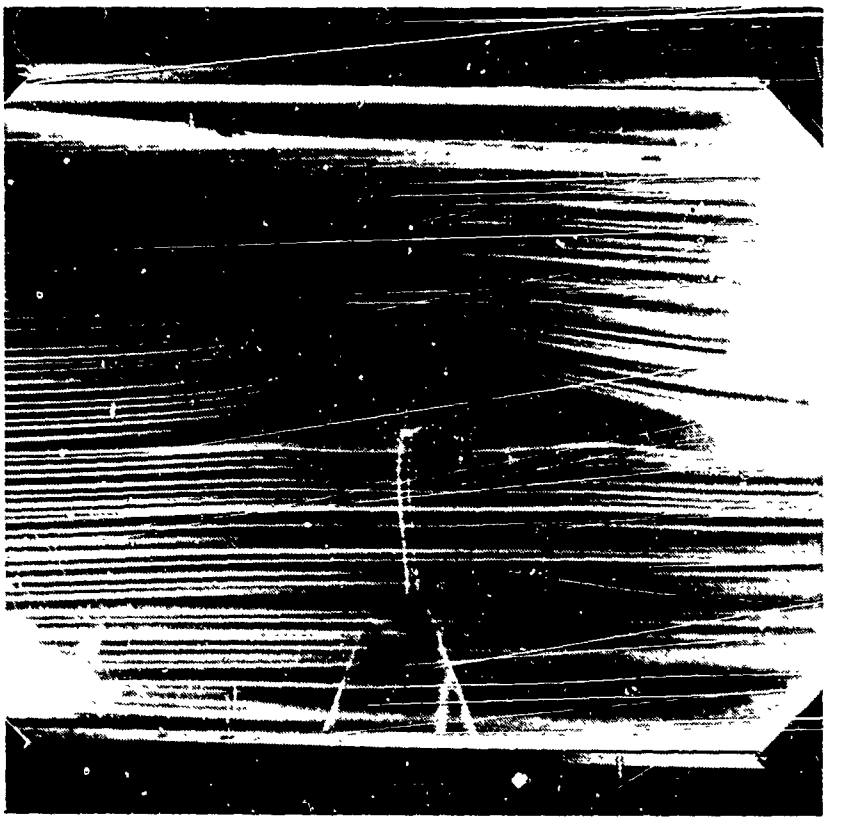

Unpowered

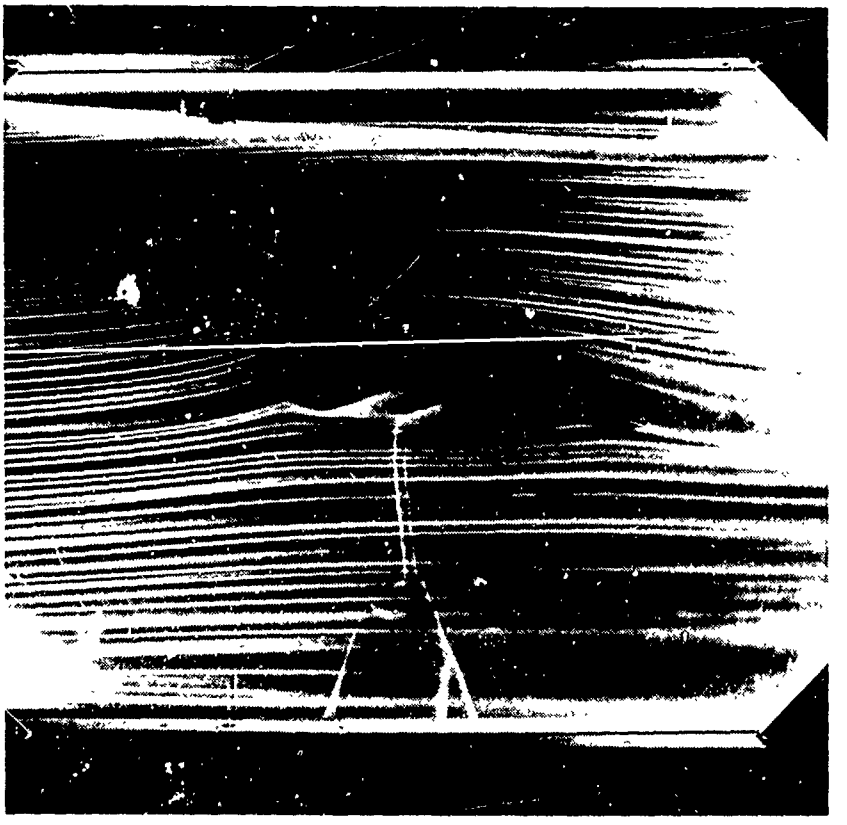

Powered

Figure 5. Flow Visualization for $\alpha = 5^{\circ}$.

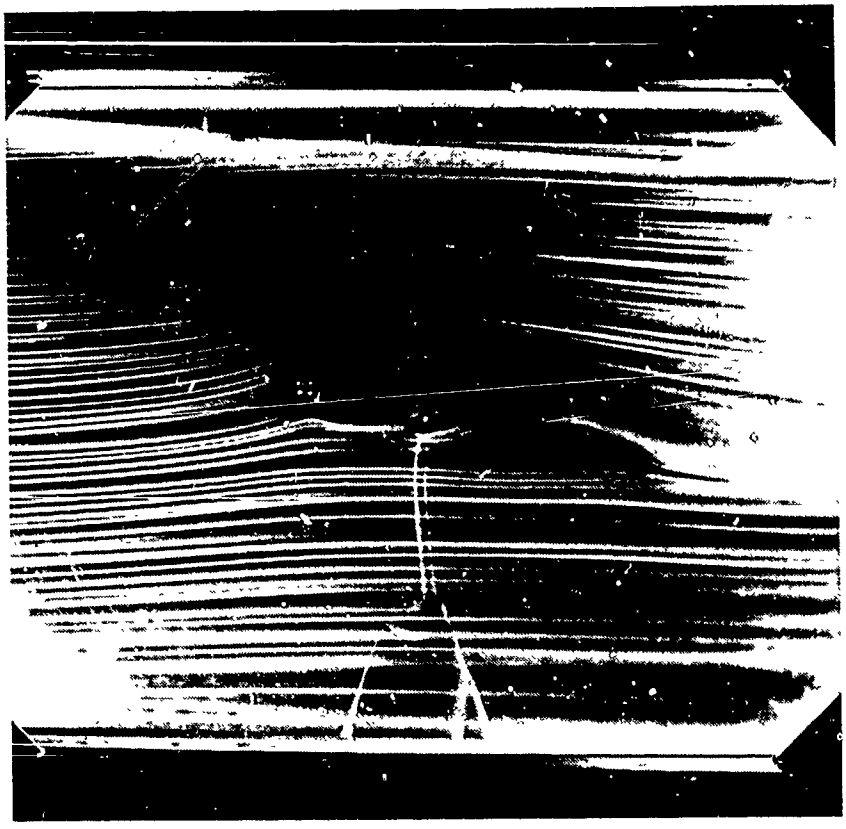

Unpowered

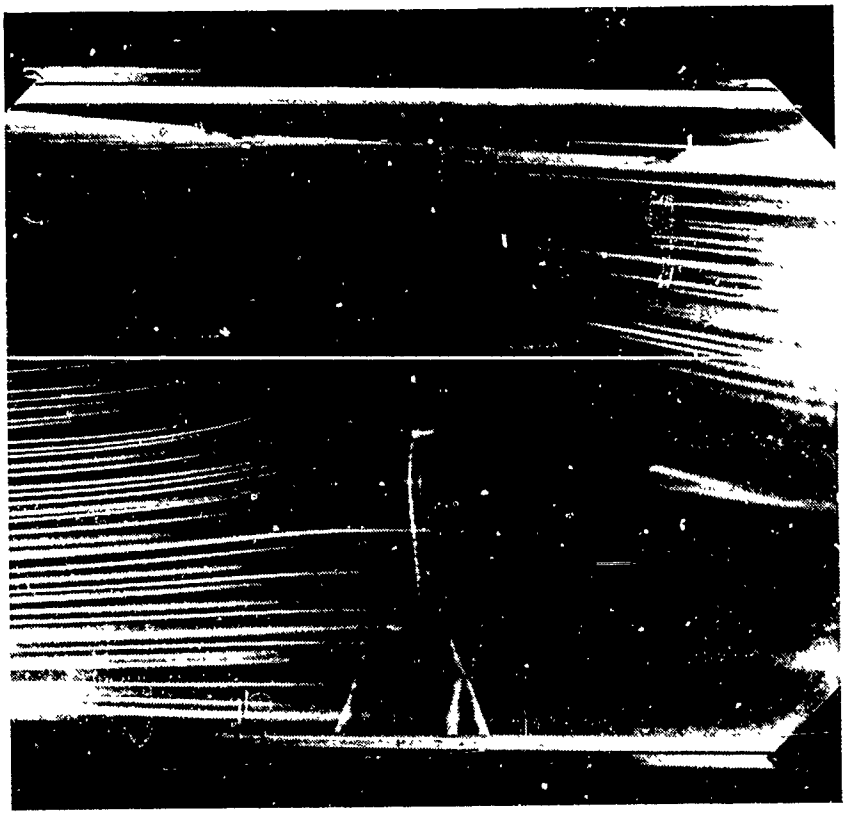

Powered

Figure 6. Flow Visualization for $\alpha = 10^{\circ}$.

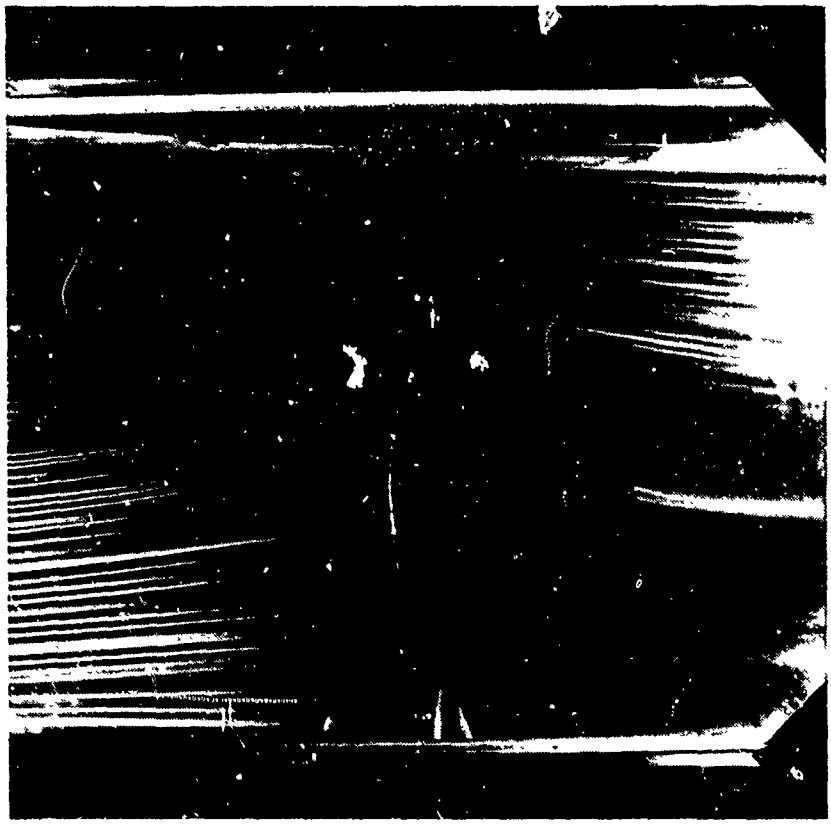

Unpowered

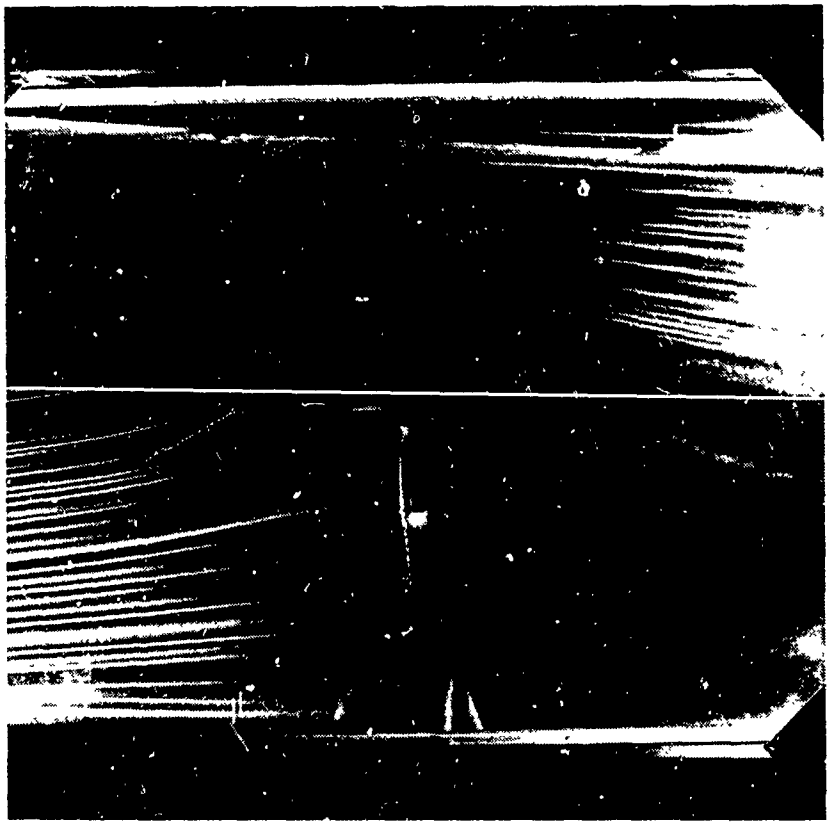

Powered

Figure 7. Flow Visualization for $\alpha = 15^{\circ}$

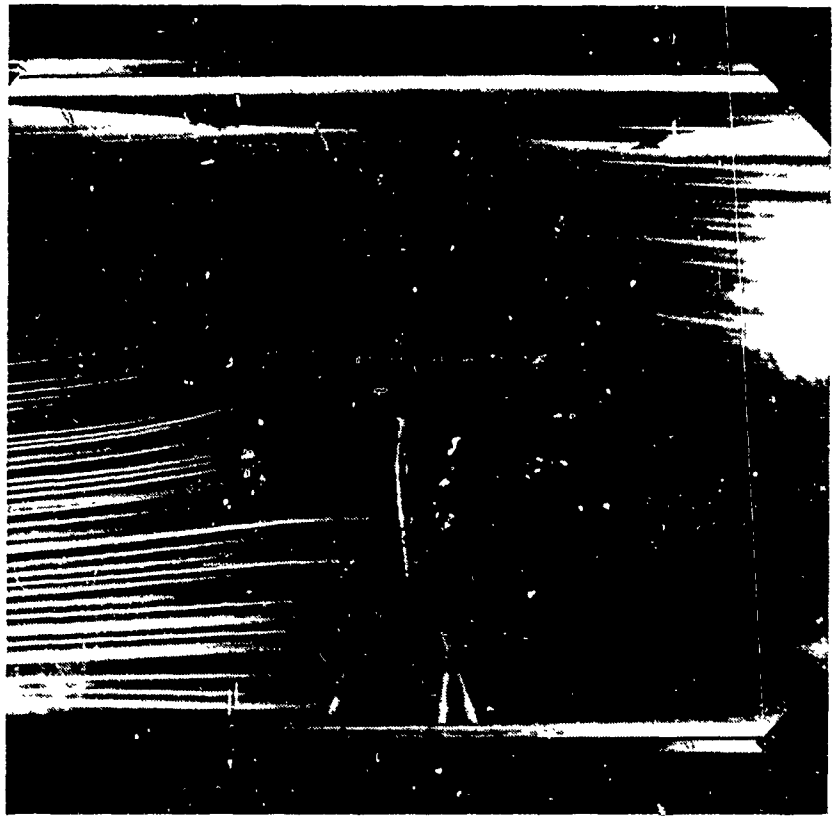

Unpowered

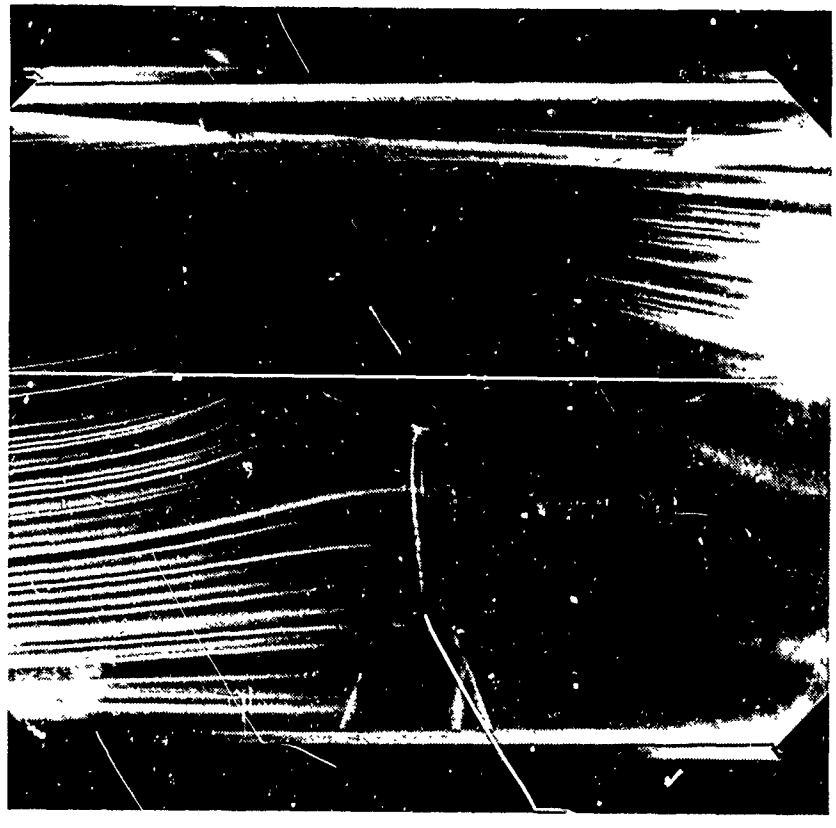

Powered

Figure 8. Flow Visualization for $\alpha = 20^{\circ}$.

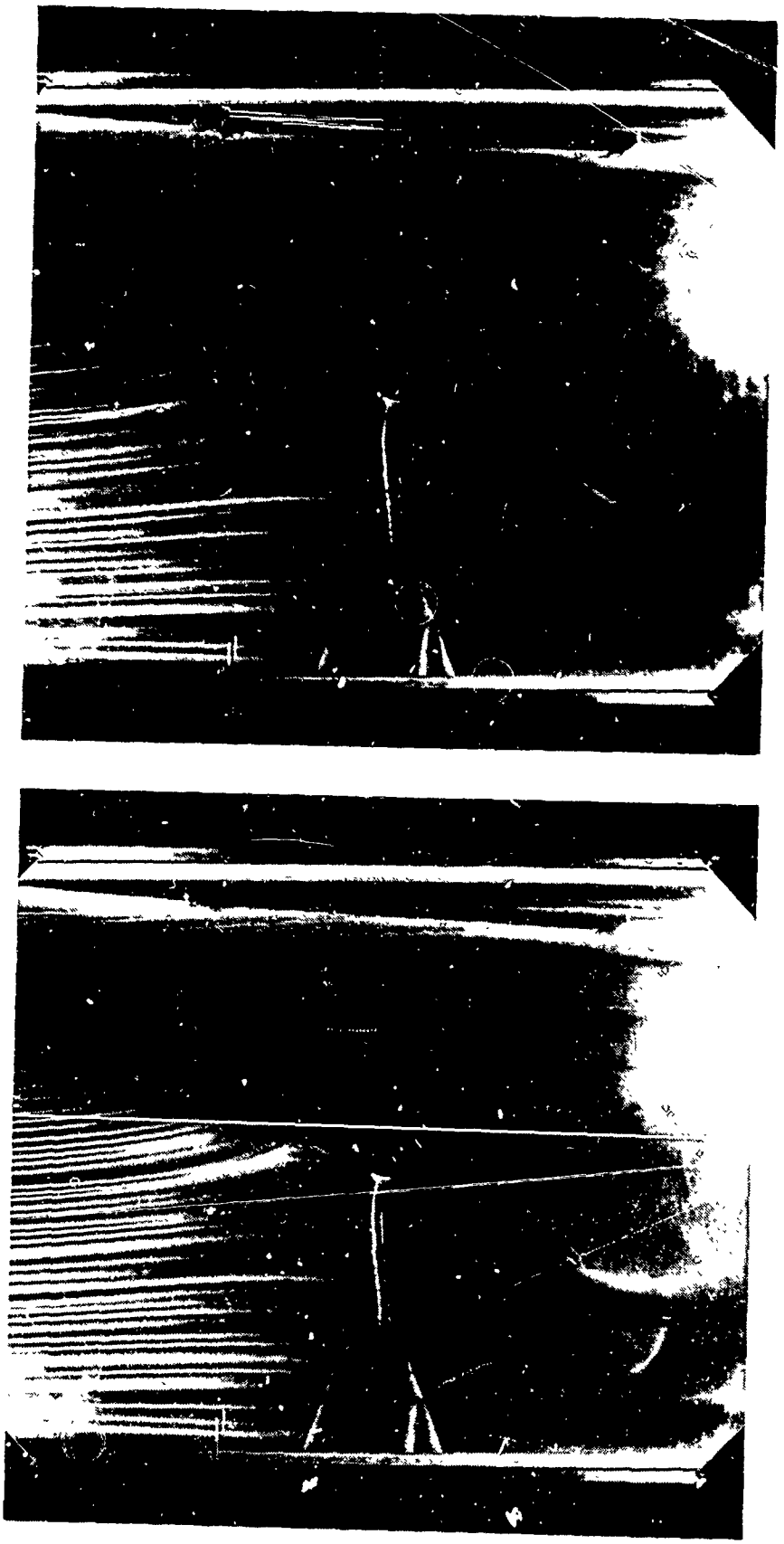

Figure 9. Flow Visualization for $\alpha = 25^{\circ}$.

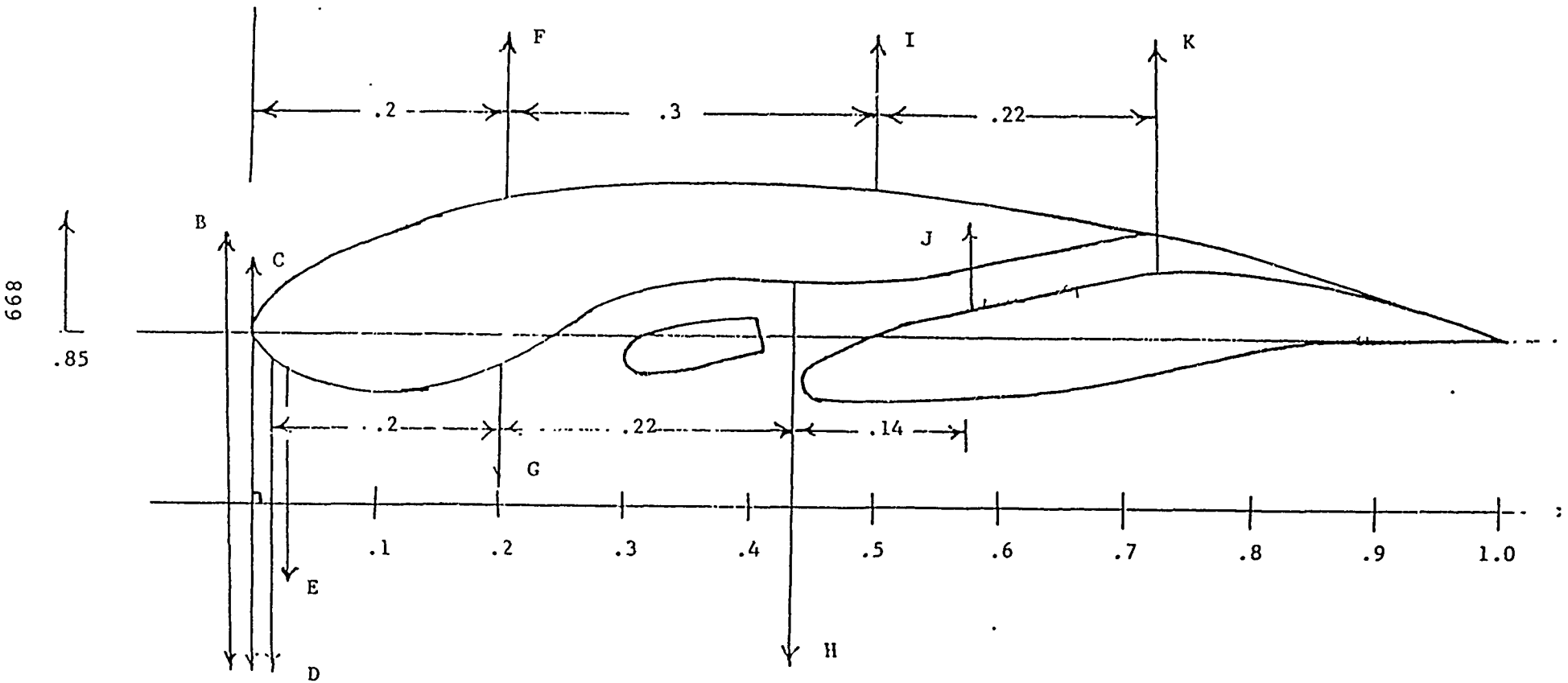

Figure 10. Measurement Locations for Ejector Wing Flow Field

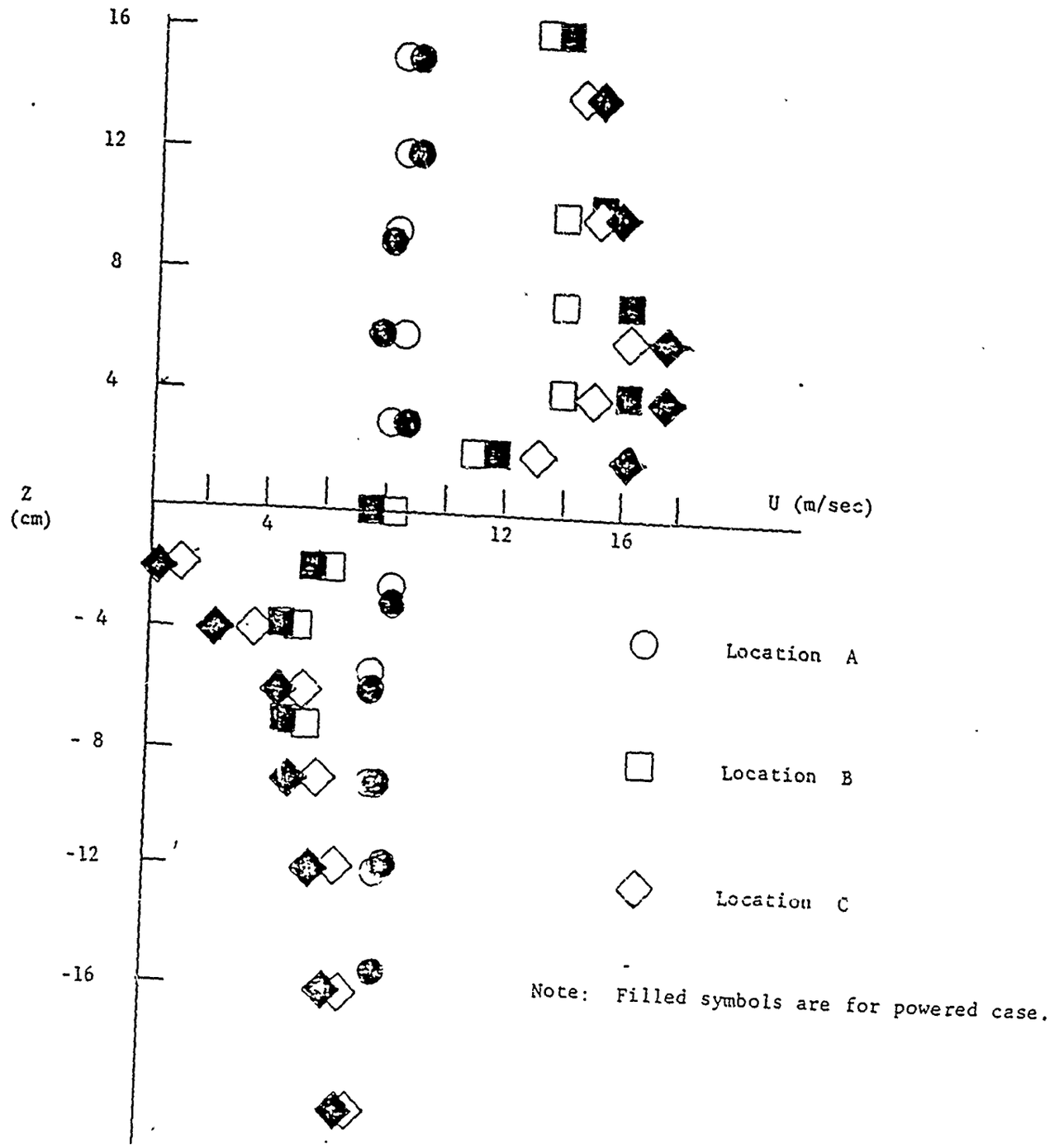

Figure 11. Mean Velocity Profiles for Ejector Wing.

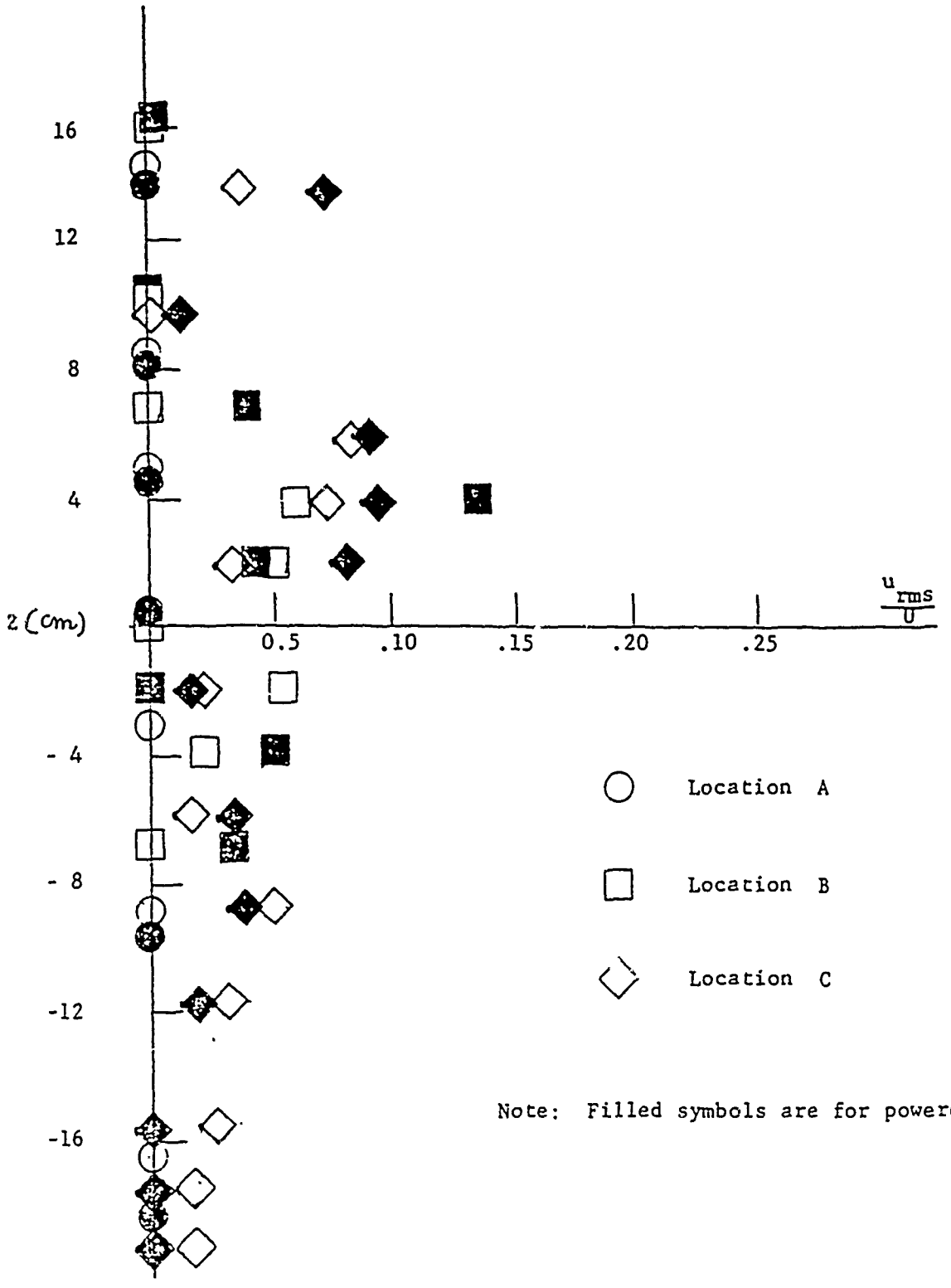

Figure 12. Turbulent Intensity Profiles for Ejector Wing.

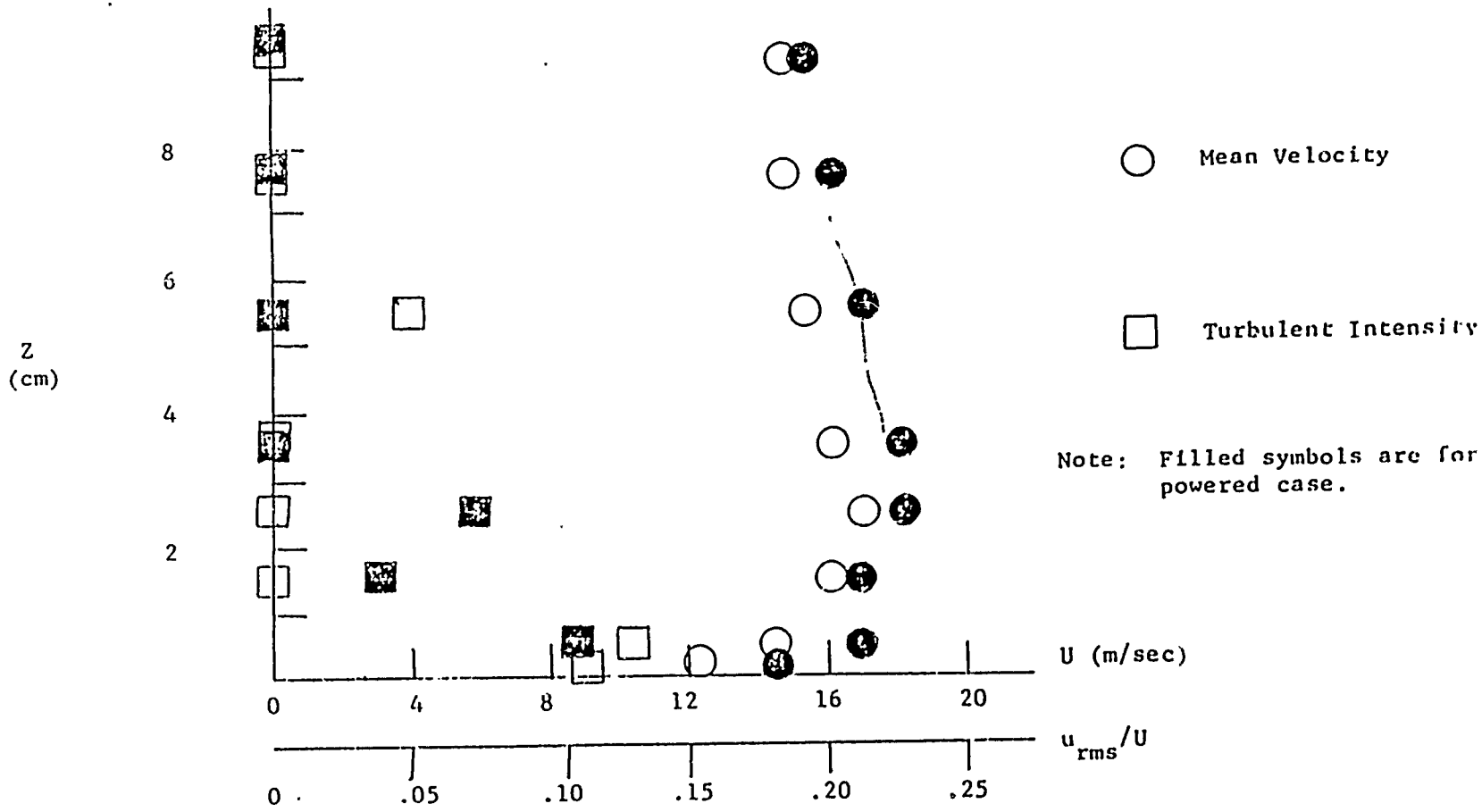

Figure 13. Mean Velocities and Turbulent Intensities at Location x/c = 0.2 (F).

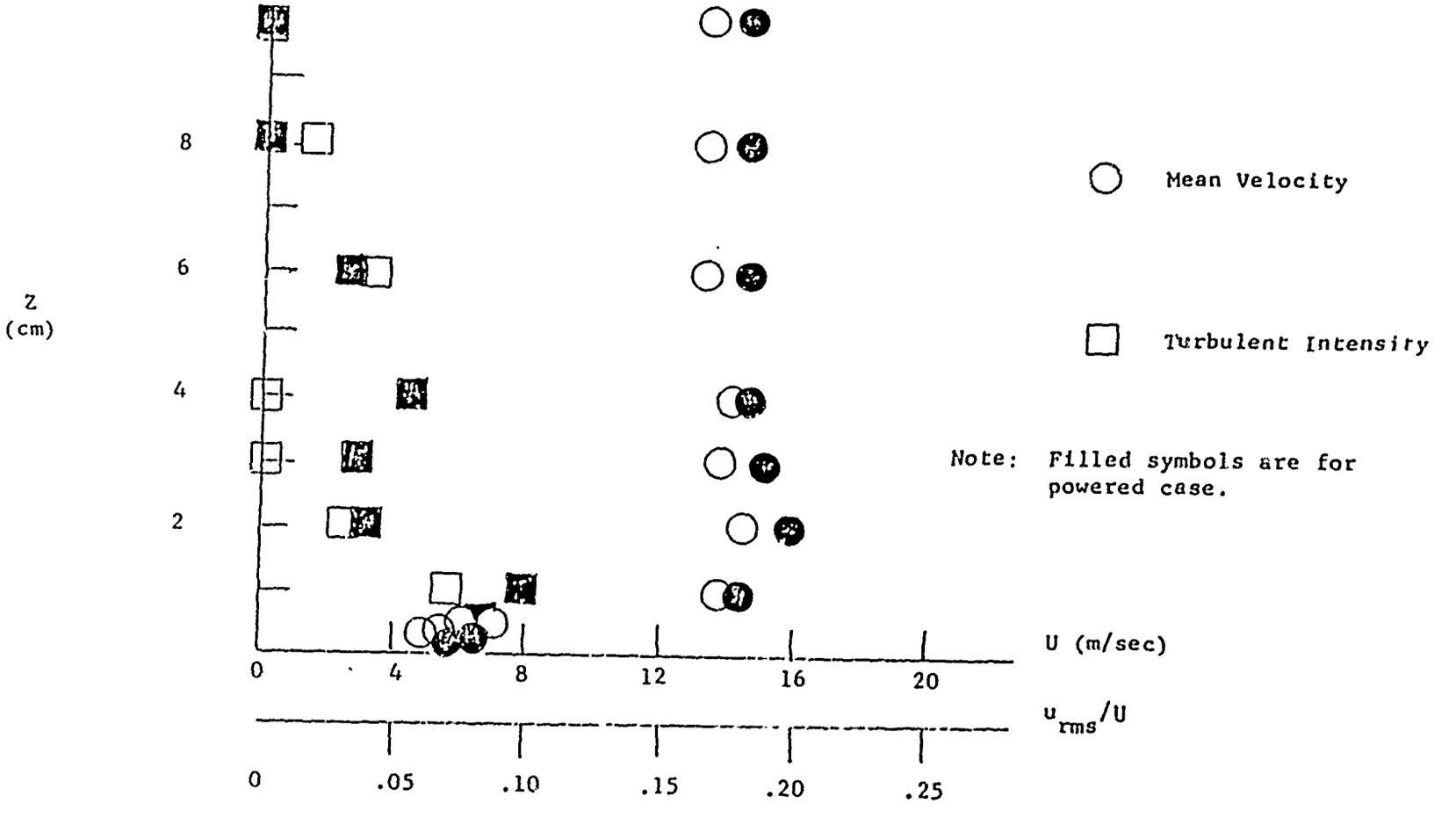

Figure 14. Mean Velocities and Turbulent Intensities at Location x/c = 0.5 (I).

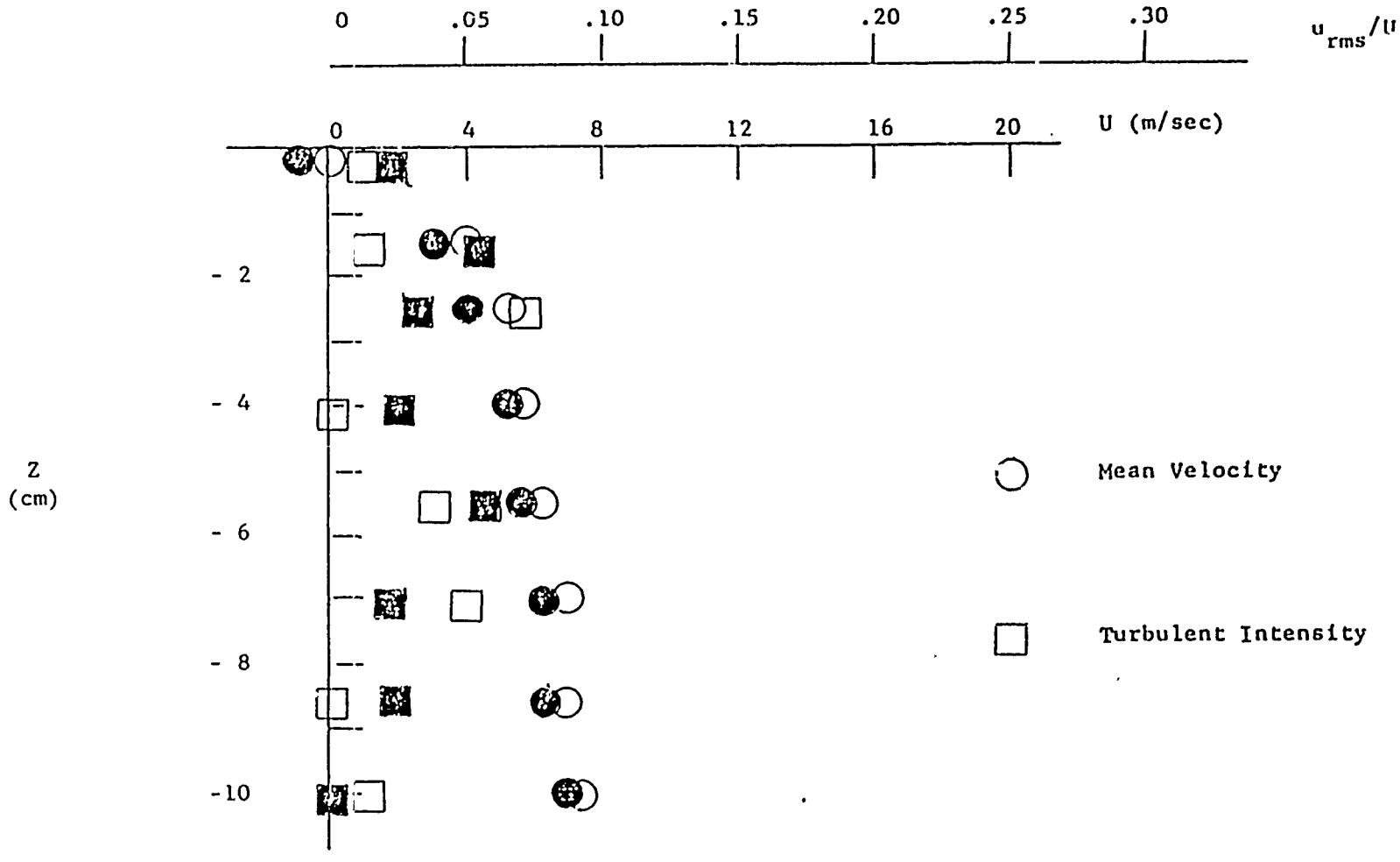

Figure 15. Mean Velocities and Turbulent Intensities at Location x/c = .02 (D).

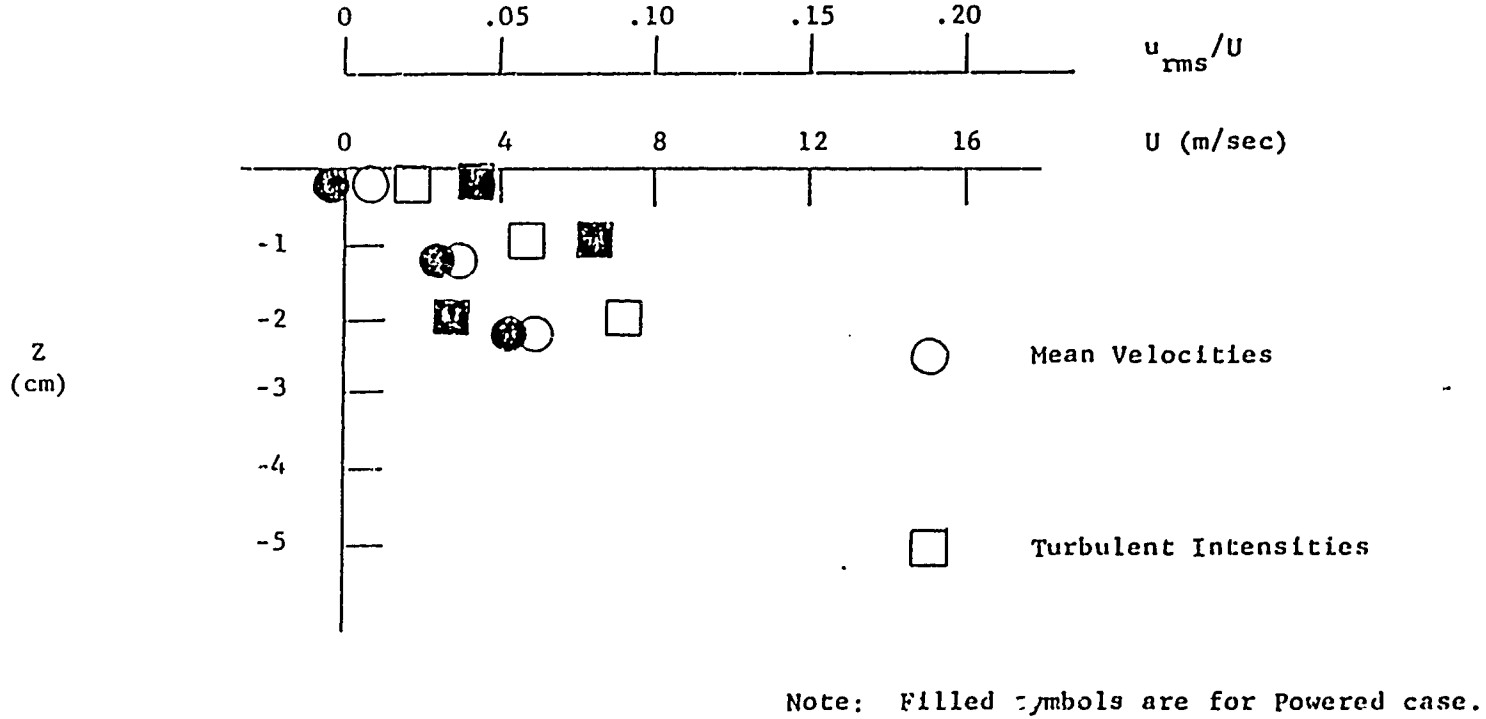

Figure 16. Mean Velocities and Turbulent Intensities at Location x/c = .04 (E).

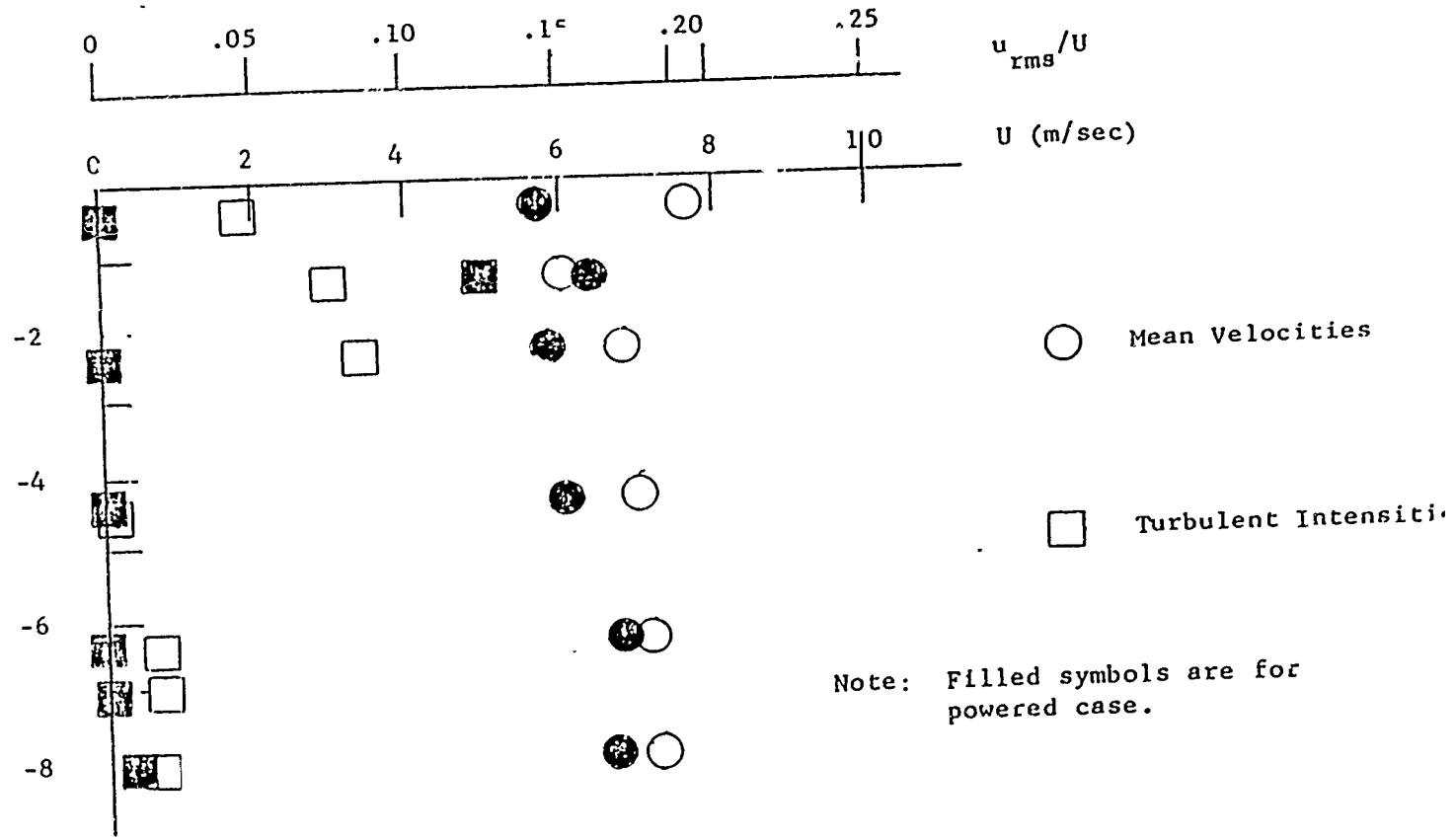

Figure 17. Mean Velocities and Turbulent Intensities at Location x/c = 0.2 (G).

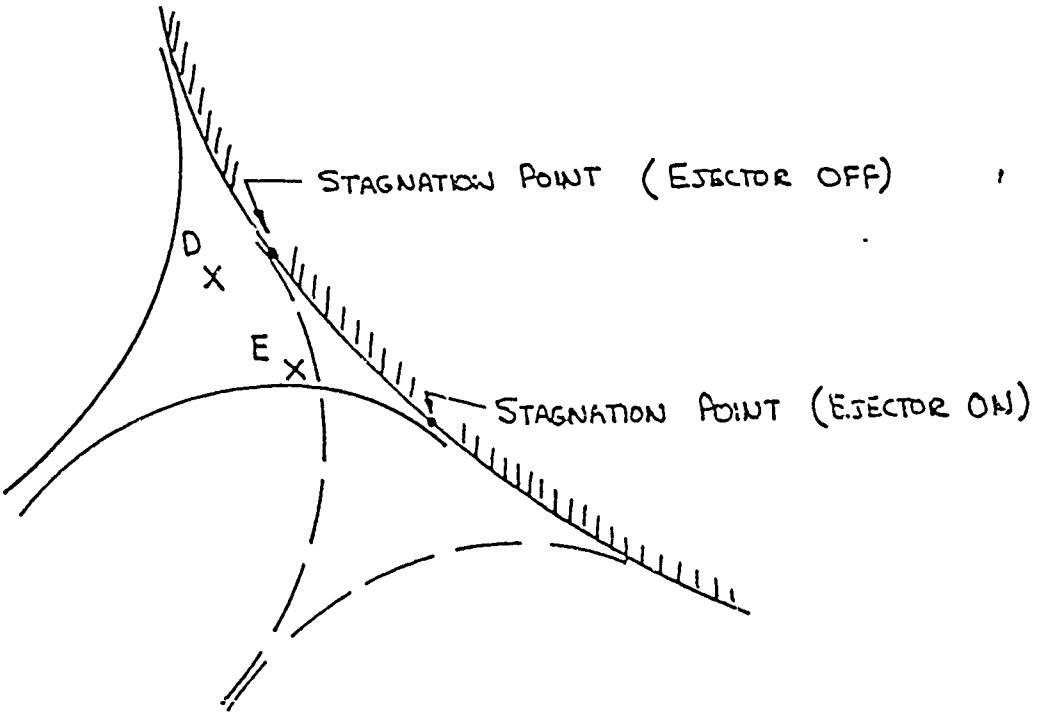

Figure 18. Shift of Stagnation Point Location Caused by Powered Ejector.

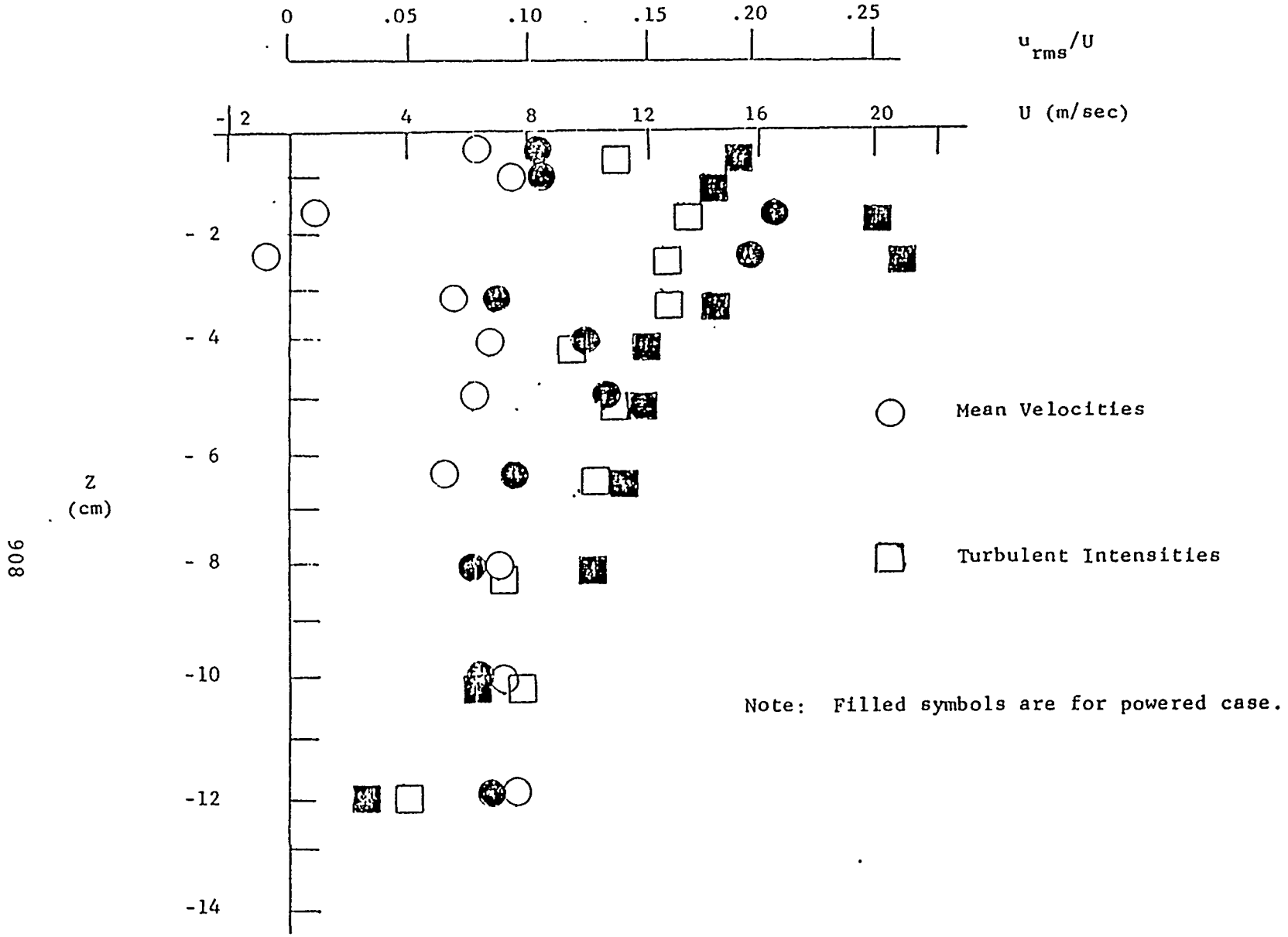

Figure 19. Mean Velocities and Turbulent Intensities at Location x/c = 44 (H).

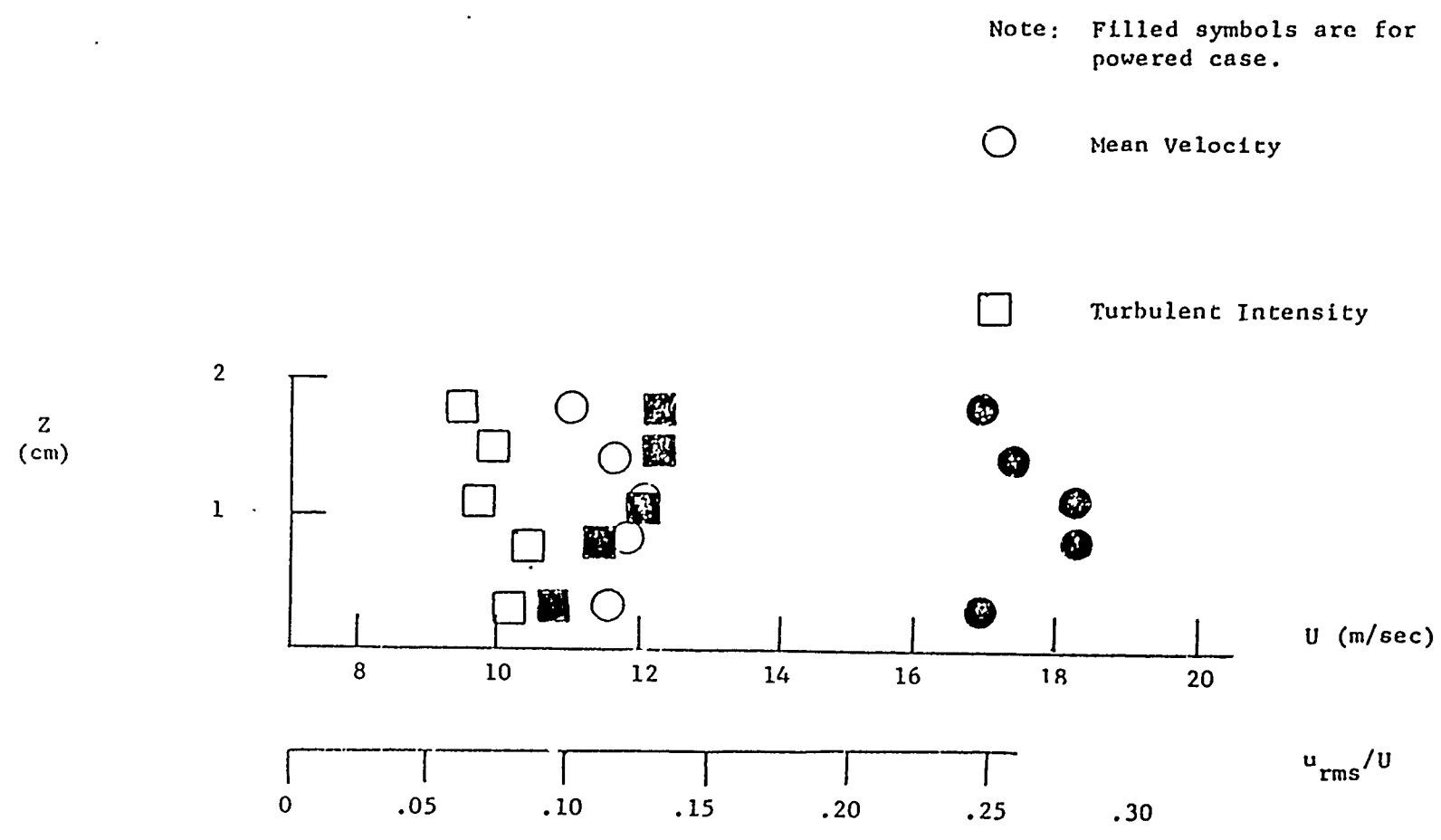

Figure 20. Mean Velocities and Turbulent Intensities at Location x/c = .58 (J).

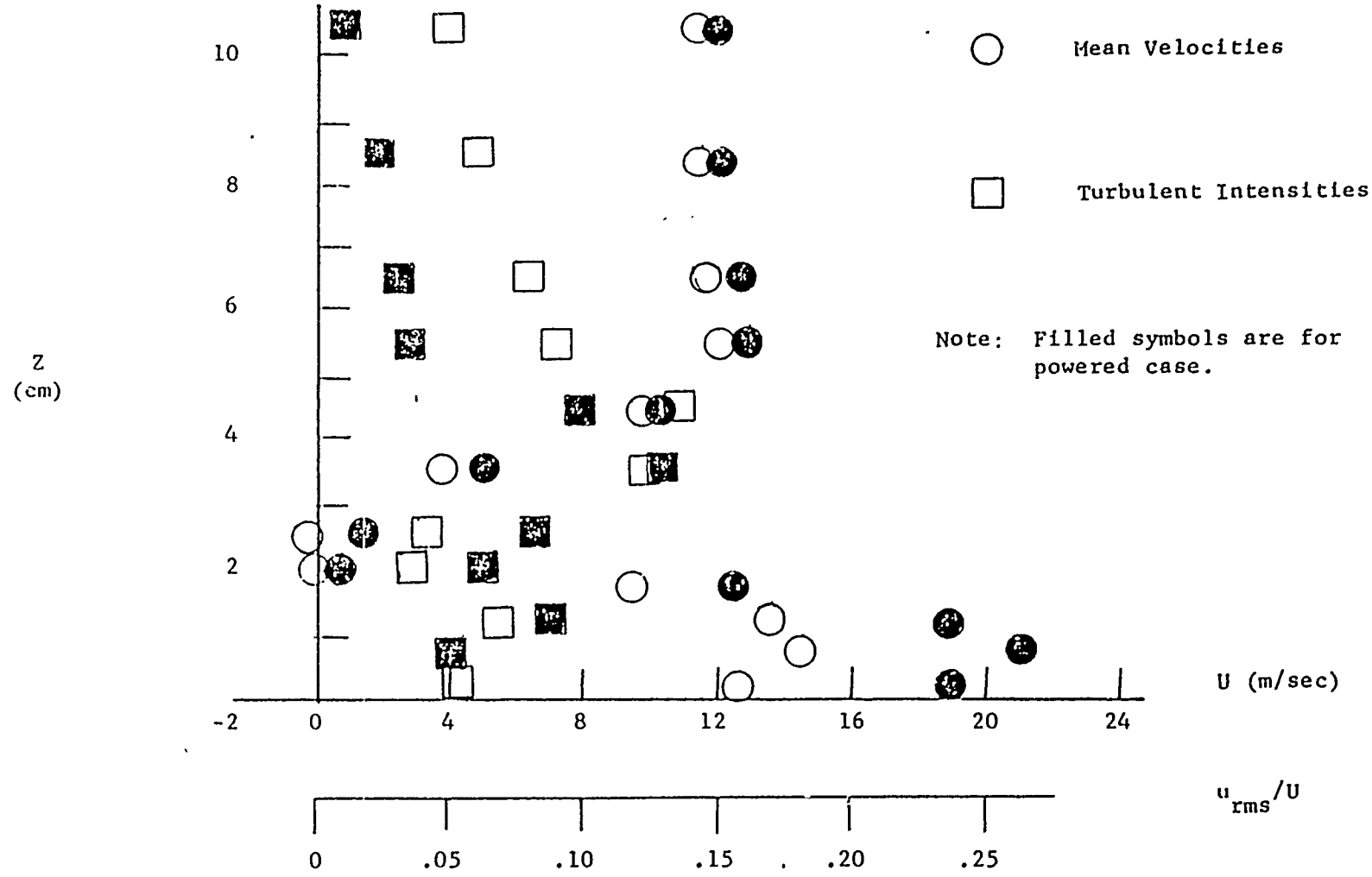

Figure 21. Mean Velocities and Turbulent Intensities at Location x/c = .72 (K).